International Core Journal of Engineering Volume 7 Issue 4, 2021
ISSN: 2414-1895 DOI: 10.6919/ICJE.202104_7(4).0064

Common Mode Inductor Selection and Test Analysis of EMI Filter for Switching Power Supply

Minyi Tao[1], Minchao Huang[2] and Xiaowen Huang[2]

[1]Logistics Engineering College, Shanghai Maritime University, Shanghai 201306, China;

[2]Minye Information Technology Co., Ltd, Shanghai 201206 China.

Abstract

Most engineers often choose EMI filter devices by trial and error, which makes the product development cycle extend again and again. In order to shorten the research and development time and reduce the research and development cost, this paper summarizes the general rules of common mode (CM) inductor selection of EMI filter, proposes a method to complete the selection of CM inductor efficiently through the insertion loss, and analyzes and tests its filtering performance. Finally, a switching power supply is used as the electromagnetic interference (EMI) test object to verify the selection method of CM inductor core material. The results show that the insertion loss (IL) method is efficient and intuitive.

Keywords

EMI Filter; Common Mode Inductor; Insertion Loss.

1. Introduction

In modern power electronic systems, passive electromagnetic interference(EMI)filters are widely used in various switching power supplies. Power system is the main source of conducted emission and radiated emission. These EMI may cause machine failure or cause catastrophic or potential damage to electronic products. Therefore, appropriate technology must be used to reduce or eliminate the leakage hazards of these EMI.

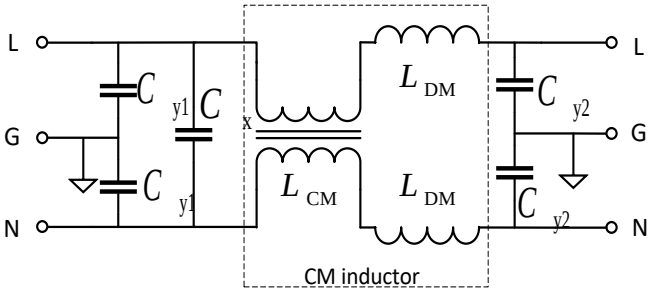

Figure 1. Typical EMI filter circuit topology

In switching mode power supply, using traditional passive EMI filter is still a good way to reduce common mode (CM) interference and differential mode (DM) interference. Figure 1 shows a typical EMI filter circuit [1], which is composed of line to line capacitance, line to ground capacitance and common mode inductance. Due to the particularity of the common mode inductor, the winding can not be completely coupled, resulting in leakage inductance. This leakage inductance can be used as differential mode inductor. The differential mode filter circuit and the common mode filter circuit can be obtained by separating the filter circuit, as shown in Figure 2. When the differential mode current is applied, the Y capacitors on the left and right sides are connected in series, and the two differential

ISSN: 2414-1895 DOI: 10.6919/ICJE.202104_7(4).0064

mode inductors are combined into one. When the common mode current is applied, the Y capacitors on the left and right sides are connected in parallel, while the X capacitors are short circuited. At this time, the filter inductance is half of the common mode inductance plus its leakage inductance. Because the leakage inductance is much smaller than the common mode inductance, the effect of leakage inductance can be ignored.

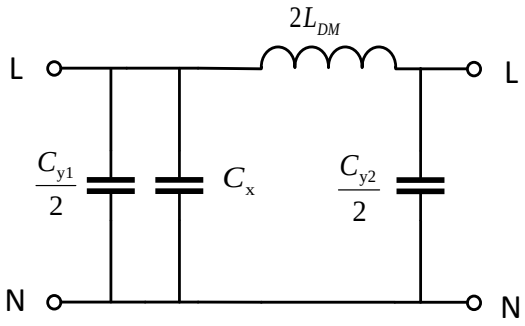

(a) Differential mode filter circuit topology

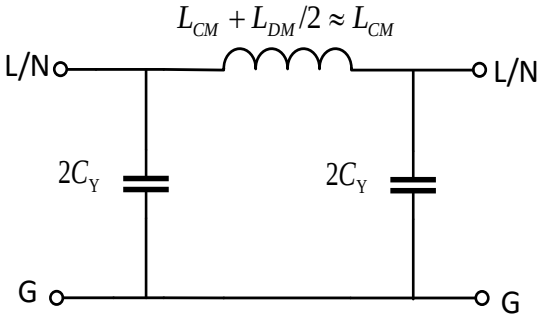

(b) Common mode filter circuit topology

Figure 2. Differential mode and common mode separation circuit

It can be seen that the suppression of noise needs to start from differential mode and common mode respectively. However, the conventional conducted interference test only tests the total noise to determine whether it is beyond the specification limit, and it is not clear about the differential mode component and common mode component in the noise, which makes it more difficult for engineers to select common mode inductor, differential mode inductor and filter capacitor. Moreover, for the common mode inductance test method, most engineers usually only have the bridge, and the frequency can only test 1kHz and 10kHz. Enterprises with better conditions will be equipped with higher bandwidth 100kHz, and a few companies will be equipped with expensive impedance analyzer. Moreover, the inductance, impedance or phase mainly measured by these instruments can not correspond to the differential mode component and common mode component needed for noise suppression, which makes the design of EMI filter at a loss. Therefore, engineers can only solve the problem by trial and error, which usually leads to over design, making the filter bulky and high cost.

For EMI filter design, common mode inductor is the most critical and complex component, which needs to consider core selection and winding design. There are many types of magnetic cores, such as silicon steel, nickel zinc, manganese zinc, iron silicon aluminum, nanocrystalline and so on. There are many kinds of winding structures, and the structures that can be mass produced are mainly parallel winding and separate winding, and the separate winding structure can be single-layer separate winding and multi-layer stacked winding. In this paper, the main winding methods, winding turns and different core materials of common mode inductors are discussed. Combined with other literatures, the selection rules of common mode inductors are summarized as follows:

(1) Winding mode: usually use parallel winding and separate winding. The leakage inductance of separate winding is larger than that of parallel winding [2], which can filter out common mode noise

ISSN: 2414-1895 DOI: 10.6919/ICJE.202104_7(4).0064

and restrain differential mode noise better than that of parallel winding; parallel winding can be used in the case of low requirements for differential mode noise suppression and strict volume requirements, and the effect of parallel winding may be better under low voltage and large current.

(2) Winding turns: theoretically, the more turns, the greater the insertion loss of common mode inductor. However, due to the influence of parasitic parameters, the insertion loss decreases with the increase of frequency [3].

(3) Core material: under the same conditions, manganese zinc has good filtering effect in the low frequency band (about 0.15-1Mhz), nickel zinc has significant filtering effect in the high frequency band (about 10-30Mhz), and nanocrystalline is prominent in the middle frequency band (about 1-10Mhz) and can have good noise suppression effect in a wide frequency band [4]. Note that the contrast frequency band is 0.15-30MHz in the conducted emission test.

According to the above selection rules, the insertion loss test method is used to verify, and the experiment shows that the selection rules are correct to a certain extent. At the same time, it also shows the intuitiveness and efficiency of the insertion loss test method. Finally, conducted interference test is carried out on a switching power supply. The EMI filter design rules are introduced, and the different conducted noise suppression effects brought by different core materials of common mode inductor are verified by experiments.

2. How to Evaluate Filter Performance

In CISPR 17, some suggestions about the test method of filter are given. There are S-parameter method, impedance method and insertion loss method. For power EMI filter, it seems unnecessary to use s parameter to evaluate its performance. The impedance can be measured directly by impedance measuring equipment, and the impedance can also be calculated by using the S parameter measured by vector network analyzer. However, the unit of EMI noise is usually expressed in dB, so it is not so intuitive to judge the noise suppression effect by impedance amplitude.

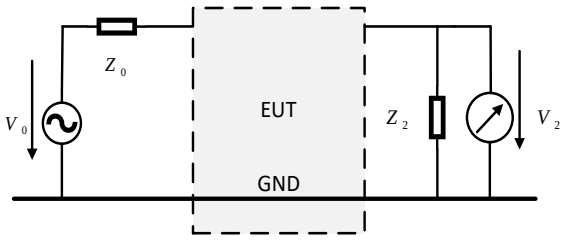

Figure 3. Insertion loss test

Insertion loss is the ratio of the voltage measured at the load end without the filter to the voltage at the load end after the filter is connected. As shown in Figure 3, the insertion loss test method is carried out under 50Ω source impedance and 50Ω load impedance, which can be calculated as follows:

$$IL = 20\,lg(V_0/2V_2) \quad (1)$$

Where IL is the insertion loss in dB, V_0 is the open circuit voltage of 50Ω signal source and V_2 is the output voltage of load terminal.

Because the insertion loss is measured in dB, the noise suppression effect in the frequency band concerned by the filter can be read directly from the insertion loss curve of the tested filter. Therefore, the insertion loss characteristics of common mode inductors will be analyzed in detail from the perspective of insertion loss.

3. Design and Selection of Common Mode Inductor

As shown in Figure 4, the EMI conducted interference test schematic diagram, EMI conducted noise includes differential mode component and common mode component. The definition of ‘differential mode voltage’ and ‘common mode voltage’ is given in the basic regulations of electromagnetic

ISSN: 2414-1895 DOI: 10.6919/ICJE.202104_7(4).0064

compatibility in CISPR 16. It can be seen from the figure that EMI conducted noise measured by EMI receiver is the sum or difference of differential mode component and common mode component. When selecting the common mode inductor, it is necessary to separate the total noise. When selecting common mode inductors, the total noise needs to be separated. In this paper, LISN (MYL16AA) with discrete differential mode and common mode function is used in Figure 5.

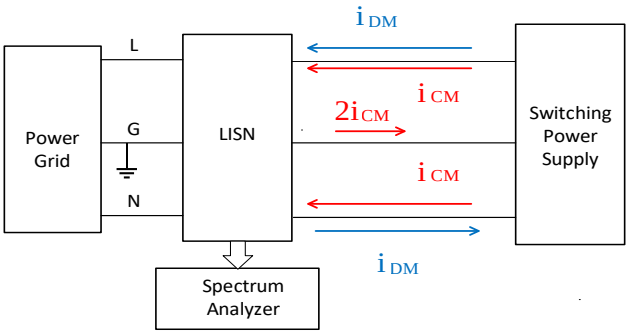

Figure 4. EMI conducted interference test

Figure 5. EMI diagnostic test system

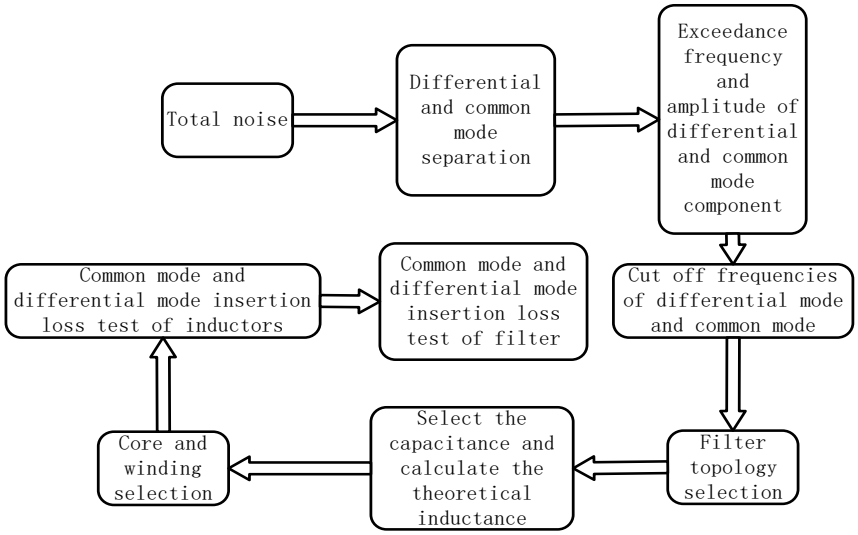

Figure 6. Common mode inductor selection steps

Figure 6 shows the design steps of common mode inductor [5,6]. The common mode inductor is not designed separately, so it needs to be considered together with the whole filter. In the design of EMI filter, the differential mode and common mode signals need to be separated. The expected insertion loss of the filter is obtained by the frequency and amplitude of the abnormal differential mode and common mode noise, and then the cut-off frequency is calculated and the topology type is selected.

ISSN: 2414-1895 DOI: 10.6919/ICJE.202104_7(4).0064

The capacitance and inductance can be calculated to select the magnetic core and winding mode. The insertion loss characteristics of the magnetic core will be described in detail in Section 3. Finally, the insertion loss of the designed common mode inductor is tested to compare whether it can achieve the expected insertion loss characteristics, and the inductance or capacitance value is adjusted appropriately. This paper will use the EMI diagnostic test system developed by Minye information technology (Shanghai) Co., Ltd. in Figure 5.

4. Insertion Loss of Common Mode Inductor

The simple equivalent circuit of the common mode inductor is shown in Figure 1. Because the split winding inductor can not be tightly wound, when the differential mode current flows through, a part of the magnetic flux will leak out, and the leakage inductance caused by this part of the magnetic flux has a certain suppression effect on the differential mode signal. Using ANSYS Maxwell 3D finite element analysis, the magnetic field density of the common mode inductor flowing through the differential mode current in Figure 7 is obtained. It can be seen that this part of the leakage flux can not be ignored.

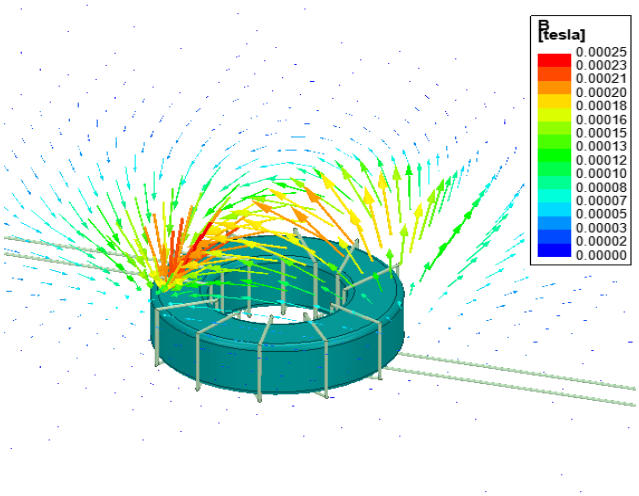

Figure 7. Magnetic field of common mode inductor excited by differential mode current

Figure 8. Three kinds of magnetic rings

The insertion loss characteristics of common mode inductors are affected by many factors, such as winding method, winding turns and magnetic material. Generally, there are two kinds of winding methods: parallel winding and separate winding. Theoretically, the more the number of winding turns, the better. However, with the increase of the number of winding turns, the parasitic parameters such as inter turn capacitance will also increase, resulting in poor high-frequency filtering effect. Manganese zinc, nickel zinc and nanocrystalline magnetic rings are the most common magnetic materials for common mode inductors. In this section, the above three factors are tested and analyzed in detail.

In this section, three magnetic rings with similar size and different magnetic materials are selected as shown in Figure 8. From left to right, they are manganese zinc magnetic ring, nickel zinc magnetic ring and nanocrystalline magnetic ring.

ISSN: 2414-1895 DOI: 10.6919/ICJE.202104_7(4).0064

4.1 Separate Winding and Parallel Winding

(a) Separate winding (left) and parallel winding (right)

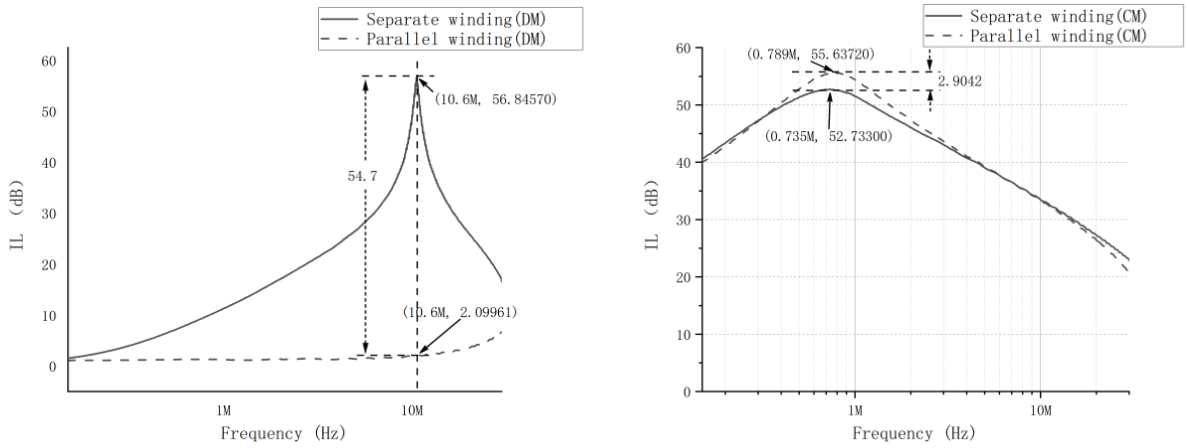

(b) Separate winding (left) and parallel winding (right)

Figure 9. Comparison of DM IL (left) and CM IL (right)

Select the MnZn magnetic ring and wind 40 turns of common mode inductor by separate winding and parallel winding, as shown in Figure 9a. The left side is separate winding and the right side is parallel winding. Through the comparison of 10b, it can be concluded that under the condition of the same magnetic material and number of turns, the difference of differential mode insertion loss between split winding and parallel winding is as high as 54.7dB at 10.6Mhz. This is due to the tight parallel winding, the leakage inductance is greatly reduced, and the suppression effect on the differential mode current is reduced. However, for common mode current, the maximum difference between separate winding and parallel winding is only 2.9dB, which can be ignored.

Therefore, the common mode inductor is usually wound by the separate winding method, which can filter the common mode noise and suppress the differential mode noise. However, this is not absolute. The inductance values of the two groups of windings of the separated common mode inductor will be slightly different. This imbalance will lead to the saturation of the magnetic core in the case of high current, resulting in the failure of the common mode inductor.

4.2 Turns

Select the nanocrystalline magnetic ring, use the separate winding method, respectively wind 20 turns, 30 turns and 40 turns for insertion loss comparison, as shown in Figure 10. It can be seen from figure 10b that every 10 turns of coil decrease will make the insertion loss curve of common mode inductor before 3MHz shift down about 6dB, and the insertion loss will be closer with the increase of frequency. Under the same magnetic material and winding method, the more the number of turns, the greater the insertion loss of the common mode inductor. However, the increase of the number of turns will lead to the increase of the inter turn capacitance. With the increase of the number of turns, the resonant frequency will shift to the left. Therefore, when selecting the number of turns, we need to consider the frequency band to suppress noise and choose a compromise scheme.

ISSN: 2414-1895 DOI: 10.6919/ICJE.202104_7(4).0064

(a) 40 turns (left), 30 turns (middle) and 20 turns (right)

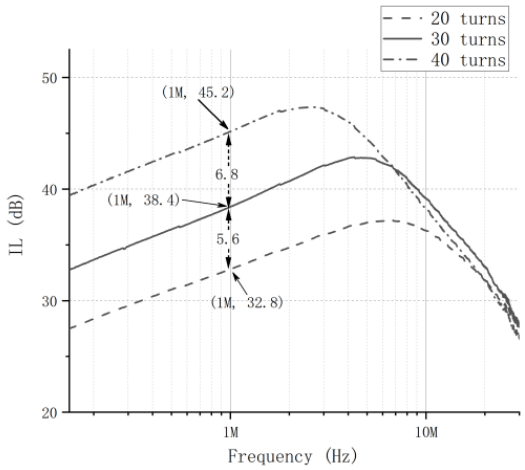

(b) Comparison of IL

Figure 10. Comparison of IL with different turns

4.3 Magnetic Materials

(a) MnZn (left), NiZn (middle) and nanocrystalline (right) CM inductors

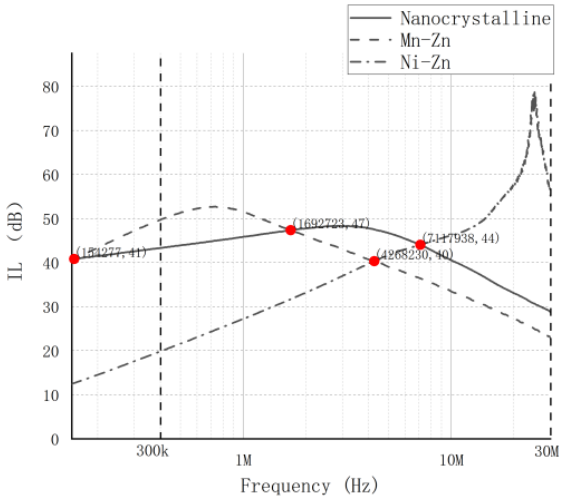

(b) Comparison of IL

Figure 11. Comparison of IL with different magnetic materials

ISSN: 2414-1895 DOI: 10.6919/ICJE.202104_7(4).0064

Select 40 turns of winding mode, respectively use MnZn magnetic ring, NiZn magnetic ring and nanocrystalline magnetic ring for IL comparison, as shown in Figure 11. Mark the frequency points 300kHz and 30MHz in Figure 11b to get the corresponding IL values, as shown in Table 1. According to the chart, the performance of MnZn magnetic ring is better in low frequency band, and the IL decreases rapidly in medium and high frequency band; on the contrary, the IL of NiZn magnetic ring is large in high frequency band, but the effect is not good in low frequency band; the insertion loss characteristics of nanocrystalline magnetic ring in medium frequency band are relatively good, and have a wide frequency band, and low, medium and high frequency have good IL characteristics. Among them, the IL of MnZn magnetic ring is the largest at 0.15~1.7Mhz; the IL of nanocrystalline ring is the largest at 1.7~7.1MHz; and the effect of MnZn magnetic ring is the best at 7.1~30MHz or even higher frequency. The IL characteristics of each kind of magnetic material are different, so the selection of CM inductance magnetic material needs to be fully weighed.

It should be noted that the above IL tests are conducted when the source impedance and load impedance are both 50Ω, while the real noise source impedance and grid side impedance are difficult to determine. Although the above common mode inductor IL characteristics are not completely accurate, they are very useful for reference.

Table 1. Comparison of IL between 300 kHz and 30 MHz

Frequency	MnZn	NiZn	Nanocrystalline
300KHz	47.32(dB)	17.67(dB)	42.58(dB)
30MHz	22.77(dB)	54.89(dB)	28.64(dB)

5. Experimental Verification

5.1 EMI Filter Design

In the third section, the selection steps of CM inductor are described. In this section, EMI conduction test is carried out for a switching power supply, and the selection method is introduced in detail. As shown in Figure 12 is the test environment, and the part marked in the red box is the EMI filter of the power supply.

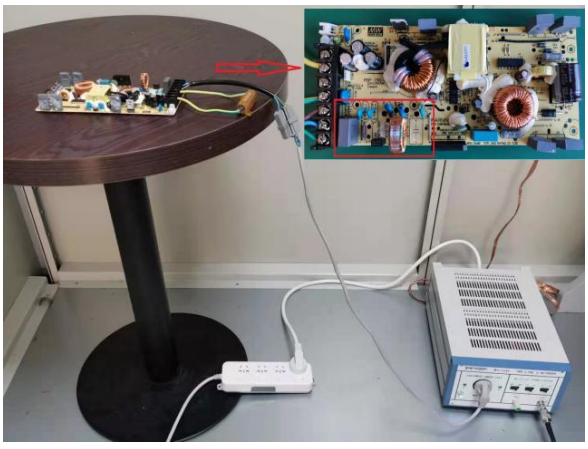

Figure 12. Conducted interference test

The total noise of the switching power supply and the DM and CM noise after separation are measured. As shown in Figure 13, the conducted interference noise of the switching power supply without filter is shown. According to equation (2), the expected IL curves of DM and CM corresponding to figure 14 are obtained through the separated DM and CM noise and standard limits, in which 3dB is the engineering margin. The standard limit is the average limit in class B of CISPR 32.

$$V_{\text{req}}(dB) = V_{measure} - V_{standard} + 3dB \quad (2)$$

ISSN: 2414-1895 DOI: 10.6919/ICJE.202104_7(4).0064

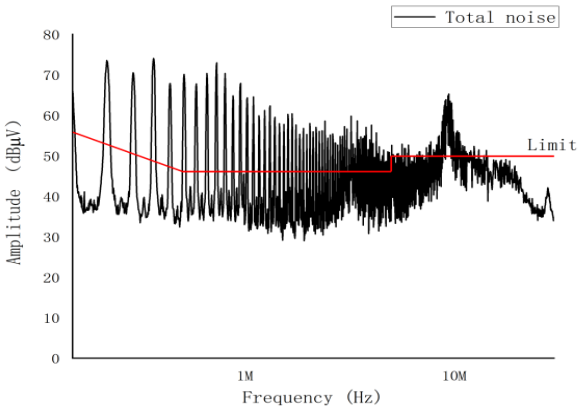

Figure 13. Conducted interference noise without filter

The EMI filter uses the topology described in Section 1. In Figure 2a, since the value of Y capacitance is much smaller than that of X capacitance, it can be ignored for simplifying the calculation. In this case, the DM filter circuit is equivalent to a second-order filter circuit, and its noise attenuation characteristic is 40dB/Dec. The CM filter circuit in Figure 2b is a third-order filter circuit with a noise attenuation characteristic of 60dB/Dec. As shown in Figure 14, the line of 60dB/decade and 40dB/decade is tangent to the expected CM IL and the expected DM IL respectively, and the frequency at the intersection point of 0 dBμV axis is the cut-off frequency. The CM cut-off frequency $f_{CCM} = 74\text{k}Hz$ and DM cut-off frequency $f_{CDM} = 58\text{k}Hz$ are obtained.

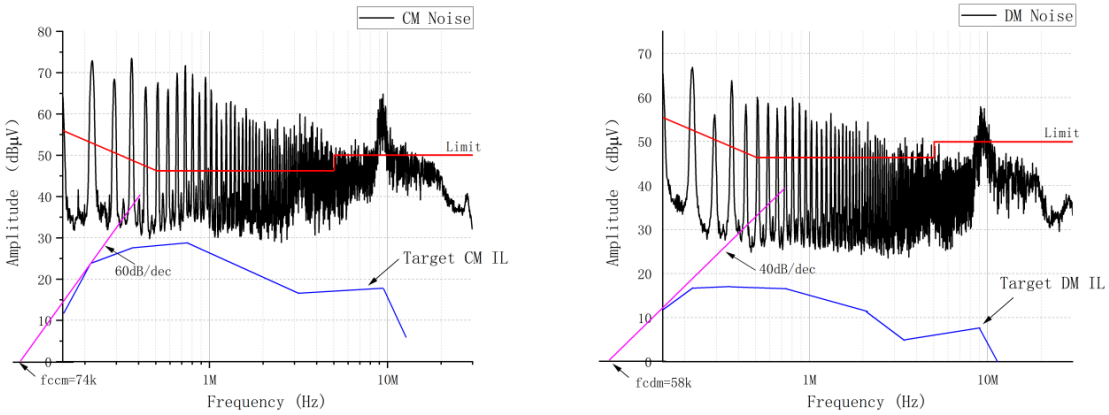

Figure 14. Expected CM (left) and DM (right) IL

According to the CM CLC filter circuit (Fig. 2b), the cut-off frequency [7] is expressed in formula (3). In order to prevent large leakage current, if the empirical value of capacitance is 1nF, the CM inductance can be calculated as 4.6mH. Similarly, according to the DM LC filter circuit (Fig. 2a), the cut-off frequency is equation (4), where the X capacitor takes the empirical value $0.47\mu F$, and the DM inductance is calculated to be $8.0\mu H$. Table 2 shows the calculated filter parameters, and the components are selected according to the parameters in the table. The DM inductance is obtained by using MnZn magnetic ring and winding separately. The calculated theoretical value is different from the actual inductance value, so it needs to be adjusted in practice.

$$f_{CCM} = \frac{1}{2\pi}\sqrt{\frac{2}{L_{CM}C_Y}} \tag{3}$$

$$f_{CDM} = \frac{1}{2\pi\sqrt{L_{DM}C_X}} \tag{4}$$

ISSN: 2414-1895 DOI: 10.6919/ICJE.202104_7(4).0064

Table 2. Filter parameters

Components	Calculated Value
L_{CM}	4.6mH
L_{DM}	8.0μH
C_X	0.47μF
C_Y	1nF

Finally, the whole filter is applied to the switching power supply to verify the whole filter design method. Figure 15 shows the conducted noise interference before and after adding filter. After adding the filter, the interference noise can be improved significantly. Because the source impedance and load impedance are both standard 50Ω in the IL test, and the impedance mismatch will appear in the actual conduction test, the EMI filter filtering effect of this test is very obvious.

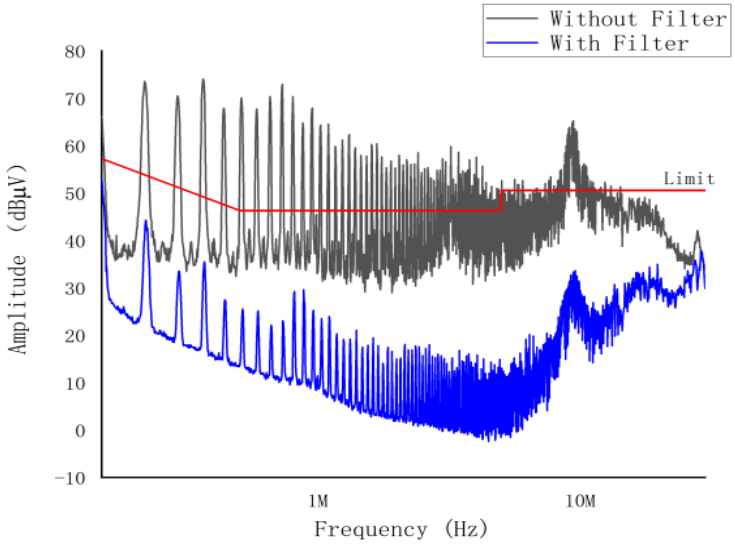

Figure 15. Comparison of total noise before and after adding filter

5.2 Conducted Interference Under Different Magnetic Materials

In this section, MnZn magnetic ring, NiZn magnetic ring and nanocrystalline magnetic ring in Section 4.3 are respectively applied to EMI filter to test EMI performance of switching power supply, and three different conducted noise characteristics in Figure 16 are obtained. Three different conductive noise characteristics in Figure 16 are obtained, and the three kinds of magnetic rings are compared in pairs. Compare the IL of the inductors corresponding to the three kinds of magnetic materials in Figure 11.

Compared with the conduction interference noise under the nanocrystalline magnetic ring and the MnZn magnetic ring, the MnZn magnetic ring noise suppression effect is better before about 2MHz, and the average noise difference is about 14dB. However, after 2MHz, the suppression effect of nanocrystalline magnetic ring is slightly better, which can be about 3dB more than MnZn. Compared with MnZn and NiZn, Ni Zn inductor has almost no filtering effect before 4MHz, and the maximum difference is about 29dB compared with Mn Zn inductor. After 4MHz, the filtering effect is very obvious, with a maximum difference of about 18dB. Compared with NiZn, the inductance of nanocrystalline is better than that of NiZn before 4MHz, with an average difference of 15dB. After 4MHz, nickel zinc is better. Table 3 shows the comparison of typical frequency points under three kinds of magnetic materials. After comprehensive comparison, the EMI filtering performance of different magnetic materials basically corresponds to the above insertion loss.

ISSN: 2414-1895 DOI: 10.6919/ICJE.202104_7(4).0064

Table 3. EMI test comparison between 0.58MHz and 6.6MHz

Frequency	MnZn	NiZn	nanocrystalline
0.58MHz	18(dBμV)	47(dBμV)	32(dBμV)
6.6MHz	22(dBμV)	32(dBμV)	19(dBμV)

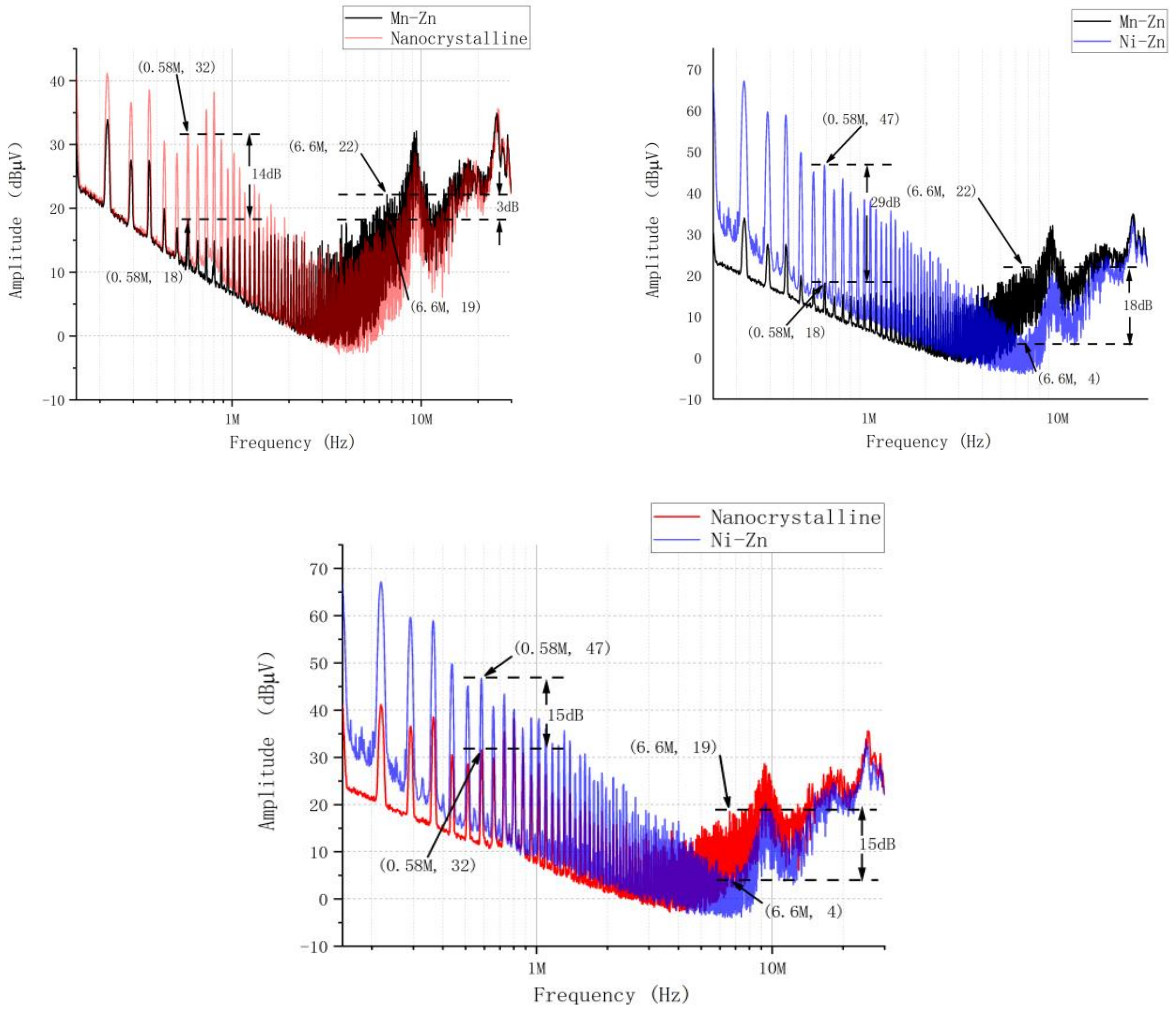

Figure 16. Comparison of conducted interference under different magnetic materials

The selection of CM inductor magnetic materials can be summarized as follows: MnZn is suitable for low frequency, NiZn is suitable for high frequency, nanocrystalline filter has a wide frequency range and is suitable for medium frequency. The experiment of conducted interference test also verifies this rule, and it also verifies that the concept of IL is a very effective way to design filters, which can help engineers design filters quickly, improve efficiency and shorten product development cycle.

6. Conclusion

Most engineers are inexperienced in the design of EMI filters. They often try and make mistakes frequently to improve EMI filters, which is time-consuming and easy to over design. In order to improve the efficiency of product design and reduce the time cost of product design, this paper summarizes the selection method of common mode inductor in passive EMI filter. Starting from the concept of insertion loss, the filtering characteristics of common mode inductor are analyzed in detail, and the influence of common mode inductor winding, turns and magnetic core on the insertion loss

ISSN: 2414-1895 DOI: 10.6919/ICJE.202104_7(4).0064

is discussed. Finally, the EMI filter design method is introduced and the magnetic material selection rule of common mode inductor is verified through the conducted interference test of a switching power supply. Experiments show that the concept of insertion loss is one of the most effective means for engineers to improve the efficiency of R & D. However, in the actual design of the filter, the near-field coupling caused by PCB wiring and EMI filter placement will make the design process seem irregular [7]. Therefore, how to solve the problem of near-field interference and make EMI filter give full play to its filtering ability is the research direction in the future.

References

[1] S. Zheng, S. Wang and B. -L. Li, "The application of multi-stage EMI filter design method in planar EMI filter," 2015 Asia-Pacific Symposium on Electromagnetic Compatibility (APEMC), Taipei, Taiwan, 2015, pp. 140-143, doi: 10.1109/APEMC.2015.7175231.

[2] R. Ren, Z. Dong, B. Liu and F. Wang, "Leakage Inductance Estimation of Toroidal Common-mode Choke from Perspective of Analogy between Reluctances and Capacitances," 2020 IEEE Applied Power Electronics Conference and Exposition (APEC), New Orleans, LA, USA, 2020, pp. 2822-2828, doi: 10.1109/APEC39645.2020.9124111.

[3] Y. Li, J. Yao and S. Wang, "Increase High Frequency Impedance of Ferrite Toroid Inductors Based on Electromagnetic Energy Analysis," 2019 IEEE Energy Conversion Congress and Exposition (ECCE), Baltimore, MD, USA, 2019, pp. 6184-6191, doi: 10.1109/ECCE.2019.8912206..

[4] C. CUELLAR and N. IDIR, "Design of Coupled Common-Differential Inductors for EMI filters," 2019 IEEE 28th International Symposium on

[5] H. Kim et al., "A new asymmetrical winding common mode choke capable of attenuating differential mode noise," 8th International Conference on Power Electronics - ECCE Asia, Jeju, Korea (South), 2011, pp. 440-445, doi: 10.1109/ICPE.2011.5944574.

[6] B. Narayanasamy, H. Jalanbo and F. Luo, "Development of software to design passive filters for EMI suppression in SiC DC fed motor drives," 2015 IEEE 3rd Workshop on Wide Bandgap Power Devices and Applications (WiPDA), Blacksburg, VA, USA, 2015, pp. 230-235, doi: 10.1109/ WiPDA. 2015. 7369320.

[7] J. Yao, S. Wang and Z. Luo, "Near Field Coupling's Impact on Radiated EMI and Mitigation Techniques for Power Converters in Automotive Applications," 2020 IEEE Energy Conversion Congress and Exposition (ECCE), Detroit, MI, USA, 2020, pp. 5882-5889, doi: 10.1109/ECCE44975.2020. 9236287.